

Optical Properties and Band Structure of Group IV-VI and Group V Materials*

MANUEL CARDONA

RCA Laboratories, Princeton, New Jersey

AND

D. L. GREENAWAY

Laboratories RCA Ltd., Zurich, Switzerland

(Received 4 October 1963)

Room-temperature reflectivity measurements over the energy range 0.5 to 25 eV have been made on the lead salts PbS, PbSe, PbTe, and on SnTe and GeTe; reflection curves have also been obtained for the structurally closely related Group V semimetals As, Sb, and Bi. In addition, the lead salts were measured at 77°K in the region below 6 eV. Measurements of transmission, also in the energy range below 6 eV, both at room temperature and at 77°K were made on epitaxially-deposited thin films of the lead salts and of SnTe. The observed structure on the reflectivity and absorption curves could be analyzed in general terms by comparison with the results obtained for diamond and zinc-blende materials and in particular by comparison with a recent augmented plane-wave band structure calculation of one of the lead salts (PbTe). An analysis of the reflectivity curves for some of the materials studied, using the Kramers-Kronig relation, enabled a detailed comparison to be made of the optical constants obtained from both reflection and transmission results.

I. INTRODUCTION

MEASUREMENTS of reflectivity and absorption in the fundamental region of a semiconductor provide a direct method of observing interband transitions and studying the band structure of the material.¹⁻⁷ In practice, because of the very high absorption coefficients involved, reflectivity measurements have received the most attention in the last few years, and their value in elucidating the deep-lying energy-band schemes in the diamond and zinc-blende structures has been more than adequately demonstrated. However, relatively few fundamental reflectivity measurements have been made on semiconductors having different structures. A natural extension of the zinc-blende materials is a study of crystals having wurtzite structure, in particular these which crystallize in both forms (e.g., ZnS). Recent results on such materials⁸ indicate the close correspondence between the zinc-blende and wurtzite structures. The present work concerns materials having basically the face-centered cubic rock-salt structure. Whereas the zinc-blende lattice consists of two face-centered cubic lattices shifted by the vector $(a/4, a/4, a/4)$, the two

face-centered cubic sublattices of the rock salt are shifted by $(a/2, a/2, a/2)$ (a is the lattice constant). In view of this similarity, one might expect some similarities between the reflectivity of the zinc-blende and rock-salt materials. We have studied the reflectivity of the lead salts PbS, PbSe, and PbTe and of SnTe and shown that such similarities exist.

It is possible to draw some conclusions about the deep-lying energy-band scheme of the lead salts by comparison with the results of a recent augmented-plane-wave (APW) type band structure calculation made by Johnson *et al.*⁹ The absorption properties of evaporated epitaxial thin films of these materials have also been studied over a limited energy range, and it is shown that excellent agreement exists between the measured absorption coefficient, and that computed from the reflectivity results using the Kramers-Kronig relation. Our results are compared with the earlier absorption curves of Gibson,^{10,11} Avery¹² and Scanlon.¹³

Earlier work on evaluation of the band structure of the lead salts has largely been limited to observations associated with the lowest conduction band and highest valence band. Both direct and indirect optical transitions have been reported in all three materials.¹³ The energy difference between these absorption thresholds (~ 0.03 eV) is of the same order as the characteristic Debye energy $k_B\theta_D$, and suggests that these indirect transitions may be caused by emission or absorption of lattice phonons, and still correspond to transitions be-

* The research reported here was sponsored in part by the Advanced Research Projects Agency Materials Science Office, under Contract SD-182, and RCA Laboratories, Princeton, New Jersey.

¹ H. R. Philipp and E. A. Taft, Phys. Rev. **113**, 1002 (1959).

² M. Cardona and G. Harbeke, J. Appl. Phys. **34**, 813 (1963).

³ J. Tauc and A. Abraham, *Proceedings of the International Conference on Semiconductor Physics, Prague, 1960* (Czechoslovakian Academy of Sciences, Prague, 1961), p. 375.

⁴ M. Cardona and D. L. Greenaway, Phys. Rev. **125**, 1291 (1962).

⁵ H. Ehrenreich, H. R. Philipp, and J. C. Phillips, Phys. Rev. Letters **8**, 59 (1962).

⁶ H. Ehrenreich and H. R. Philipp, *Proceedings of the International Conference on the Physics of Semiconductors, Exeter, 1962* (The Institute of Physics and the Physical Society, London, 1962), p. 367.

⁷ M. Cardona and D. L. Greenaway, Phys. Rev. **131**, 98 (1963).

⁸ M. Cardona, Phys. Rev. **129**, 1068 (1963); also Solid-State Communications **1**, 109 (1963).

⁹ L. E. Johnson, A. C. Switendick, J. B. Conklin, and G. W. Pratt, Jr., MIT Solid-State and Molecular Theory group, Progress Report No. 46, 1962 (unpublished).

¹⁰ A. F. Gibson, Proc. Phys. Soc. (London) **B63**, 756 (1950).

¹¹ A. F. Gibson, Proc. Phys. Soc. (London) **B65**, 378 (1952).

¹² See T. S. Moss, *Optical Properties of Semiconductors* (Butterworths Scientific Publications Ltd., London, 1959), p. 188.

¹³ W. W. Scanlon, *Solid State Physics*, edited by F. Seitz and D. Turnbull (Academic Press Inc., New York, 1959), Vol. 9, p. 115.

tween valence and conduction-band extrema at the same point in the Brillouin zone. The band extrema of PbTe have previously been studied using the de Haas-van Alphen effect,¹⁴ Azbel-Kaner resonance,¹⁵ and the Shubnikov-de Haas effect.¹⁶ These experiments indicate both for the valence and conduction band the presence of four prolate ellipsoids along the $[111]$ directions with their extrema at the faces of the Brillouin zone (L point). The bands give rise to a small direct-energy gap at the edge of the Brillouin zone. The effective mass of the valence-band ellipsoids is strongly temperature-dependent due to the adding effects of nonparabolicity and the temperature variation of the energy gap; this causes an unusually steep temperature dependence of mobility in both n - and p -type PbTe. The separation of the valence-band extrema is small (de Haas-van Alphen effects give an estimate of 0.002 eV); however, recent infrared reflectivity and absorption measurements¹⁷ suggest a value of 0.08 eV. Calculations seem to show that it is unlikely that the indirect optical gap is caused by transitions from the $[000]$ valence-band maximum to the conduction band at the L point. These considerations also apply to PbS and PbSe, although there is evidence that the energy bands are nearly isotropic, i.e., the energy surfaces are nearly spherical.^{18,19} Although one may conclude from this isotropy that the direct gap occurs at $\mathbf{k}=0$, one must realize that constant energy ellipsoids at L may also be near isotropic. In view of the identical anomalous temperature coefficients of the optical gaps for the lead salts and the discussion in the following sections, it seems more reasonable to assign the optical gap to the same transition in all three materials.

There is uncertainty as to whether SnTe is a semiconductor or a semimetal. It can only be prepared as a p -type material with about 10^{20} holes $\times \text{cm}^{-3}$.²⁰ This fact favors the semimetal character of the material, however, recent measurements of thermoelectric power²¹ seem to favor the semiconductor character. Little is

known about its band structure, and consequently, SnTe has been included in the present measurements.

The Group V semimetals As, Sb, and Bi, and also the IV-VI compound GeTe, form a closely related group of materials having the rock-salt structure with the addition of a small trigonal distortion along the $[111]$ axis. Consequently, one might expect similarities in the deep-band structure with the lead-salt semiconductors. Hall and Koenig²² have demonstrated that the band structure of the Group V semimetals can be obtained from the lead-salt band structure (i.e., PbTe) by subjecting the lattice to a small uniaxial extension in the $[111]$ direction. These authors have also shown that such experimental results as the reversal of the conductivity anisotropy at low temperatures in Bi-Sb alloys can be completely predicted by this type of treatment. The Fermi surface of semimetals such as Bi has been investigated for many years, and its ellipsoidal nature is well known, but it has only recently been demonstrated that the electrons lie in three ellipsoids centered at the L point and light holes in a fourth ellipsoid.²³ There are no measurements however on the deeper lying bands and in the present work we have shown the similarities that exist between these semimetals and the lead salts.

II. MEASUREMENTS

A. Equipment

The low-energy reflectivity results (<6 eV) were obtained using a 50-cm Bausch and Lomb grating instrument, and a quartz windowed cryostat capable of being cooled to 77°K. No reference mirror was used, the photomultiplier detector being rotated around the cryostat to obtain direct and reflected intensities. The precautions taken to avoid specimen surface contamination have been described elsewhere.⁷ Low-energy absorption curves were obtained using a Cary double-beam spectrophotometer. Reflectance in the 6–25-eV region was measured with a Jarrell-Ash 1-m Seya-type spectrometer used in windowless operation. The source used, and the experimental technique is also detailed elsewhere.⁷ Owing to the relatively high gas pressure in the system during operation, reliable measurements could not be taken at low temperature in the vacuum ultraviolet. Marked changes with time were initially observed in the reflectance of both PbS and PbSe when measured using the hydrogen source. Smith and Dutton have also reported this effect²⁴ in their measurements of the photoelectric yield of PbS, but do not explain it. These effects have now clearly been shown to arise solely from a photochemical reaction involving the hydrogen gas present in the spectrometer. Replacement of the source gas by either neon, argon, or helium gave completely reproducible reflectances that showed no

¹⁴ P. J. Stiles, E. Burstein, and D. N. Langenberg, *J. Appl. Phys.* **32S**, 2174 (1961).

¹⁵ P. J. Stiles, E. Burstein, and D. N. Langenberg, *Proceedings of the International Conference on the Physics of Semiconductors, Exeter, 1962* (The Institute of Physics and the Physical Society, London, 1962), p. 577.

¹⁶ K. F. Cuff, M. R. Ellett, and C. D. Kuglin, *Proceedings of the International Conference on the Physics of Semiconductors, Exeter, 1962* (The Institute of Physics and the Physical Society, London, 1962), p. 316.

¹⁷ J. R. Dixon and H. R. Riedl, *Proceedings of the International Conference on the Physics of Semiconductors, Exeter, 1962* (The Institute of Physics and the Physical Society, London, 1962), p. 179.

¹⁸ G. L. Bir and G. E. Pikus, *Fiz. Tverd. Tela* **4**, 2243 (1962) [English transl.: *Soviet Phys.—Solid State* **4**, 1640 (1963)].

¹⁹ E. D. Palik and D. L. Mitchell, *Conference on High Magnetic Fields, Their Production and Applications*, Clarendon Laboratory, University of Oxford (unpublished).

²⁰ R. F. Brebrick and A. J. Strauss, *Phys. Rev.* **131**, 104 (1963).

²¹ R. S. Allgaier and B. B. Houston, *Proceedings of the International Conference on the Physics of Semiconductors, Exeter, 1962* (The Institute of Physics and the Physical Society, London, 1962), p. 172.

²² J. J. Hall and S. H. Koenig, *Bull. Am. Phys. Soc.* **8**, 51 (1963).

²³ A. L. Jain and S. H. Koenig, *Phys. Rev.* **127**, 442 (1962).

²⁴ A. Smith and D. Dutton, *Phys. Chem. Solids* **22**, 351 (1961).

variation with high-energy irradiation. This photochemical reaction was confirmed by the slight smell of hydrogen sulphide that existed in the specimen chamber when samples were being removed after windowless hydrogen operation.

B. Sample Preparation—Reflection

A number of etching techniques have been published for PbTe and PbS,^{17,25,26} all claim to, and in fact do, give mirror-like etched surfaces. However, we have consistently found that the reflectance maxima in the near ultraviolet from these etched surfaces occur at lower energies (up to 0.2 eV) than peaks obtained from cleaved surfaces. Surfaces used for reflectance in the present work have therefore all been either cleaved, or "as grown" in the case of the epitaxial layers. Cleaved single-crystal material was used for all the measurements below 6 eV. Measurements in the vacuum ultraviolet were obtained from cleaved single crystals in the case of As, Sb, Bi, and from evaporated epitaxial layers in the case of the lead salts, SnTe and GeTe. The layers were evaporated onto single-crystal substrates, cleaved in air, and held at a temperature of approximately 300°C. The technique followed that reported by Schoolar *et al.*²⁷; x-ray results showed all the films to be single crystal and to have the crystal orientation [in this case (100)] of the substrate. The GeTe prepared in this manner showed a polycrystalline nature and no epitaxial effect. Some attempt was made to match the lattice constants between films and substrates, though there are doubts whether this refinement is really necessary. Consequently, the following combinations were adopted: PbTe on KBr, PbSe on KCl or NaCl, PbS on NaCl, and SnTe on KCl. No attempt was made to determine the impurity levels in the materials studied; we have found for diamond and zinc-blende materials that the reflectivity spectra are not influenced by normally encountered variations in impurity concentration.²⁸

C. Transmission Measurements

Epitaxial thin films for transmission measurements were also prepared by the technique detailed above. A quartz substrate was mounted next to the alkali-halide substrate during evaporation. The optical density of both films was the same. The thickness of the films was determined on the film with the quartz substrate by the Tolansky interference method. Photographs of the step fringes produced at the layer edges enabled the thickness to be estimated with an accuracy of ± 100 Å. The layers measured in the following section had a thickness

²⁵ R. F. Brebrick and W. W. Scanlon, *J. Chem. Phys.* **27**, 607 (1957).

²⁶ P. H. Schmidt, *J. Electrochem. Soc.* **108**, 104 (1961).

²⁷ R. B. Schoolar, J. D. Jensen, and J. N. Zemel, *Bull. Am. Phys. Soc.* **8**, 63 (1963).

²⁸ M. Cardona and H. S. Sommers, Jr., *Phys. Rev.* **122**, 1382 (1961).

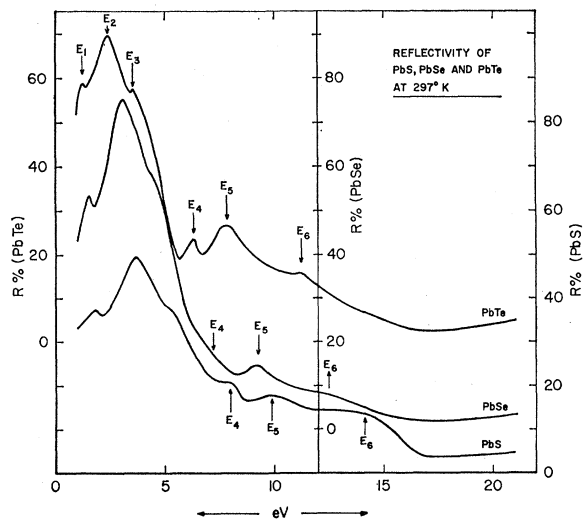


FIG. 1. Room-temperature reflectivity of PbS, PbSe, and PbTe.

of approximately 300 Å, and appeared light yellow by transmitted light. Besides measurement at room temperature and 77°K, one of the PbTe films was measured at liquid-helium temperature. No significant difference between the 77 and 4°K curves was observed except for a very slight sharpening of the structure at the lower temperature.

III. RESULTS

The room-temperature reflectivity of the three lead salts is shown in Fig. 1. Attempts were made to obtain good absolute values of the reflectivity and the curves shown should be accurate to a few percent. The corresponding results for SnTe and GeTe are shown in Fig. 2. We have labeled the reflectivity peaks E_1 to E_6 , the E_2 peak in all cases corresponds to the absolute maximum in reflectivity. It should be noted that whereas the lead salts show a rise in reflectivity at high energies (above 15 eV), SnTe and GeTe do not. This behavior is discussed in Sec. V. The E_1 , E_2 , and E_3 peaks

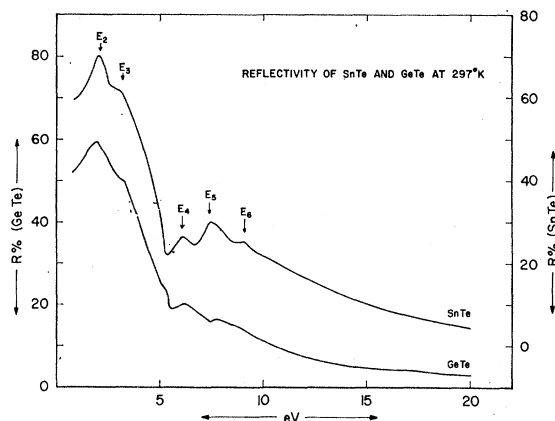


FIG. 2. Room-temperature reflectivity of SnTe and GeTe.

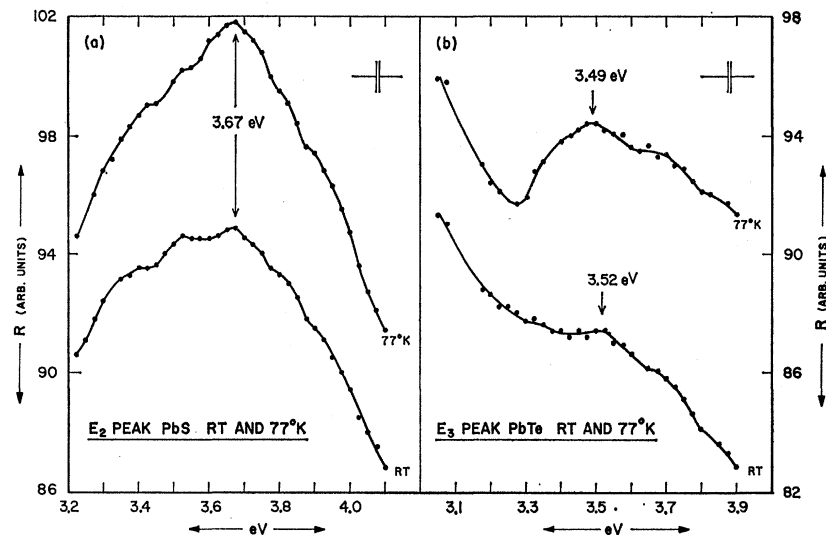


FIG. 3. (a) Reflectivity at RT and 77°K of E_2 peak in PbS. (b) Reflectivity at RT and 77°K of E_3 peak in PbTe.

in the lead salts were also examined in greater detail than is shown in Fig. 1, both at room temperature and 77°K. The reason was twofold: to establish the presence, if any, of fine structure on these peaks, and to attempt to measure the temperature coefficients. We could detect no fine structure on the E_1 , however all three lead salts showed evidence of structure on the E_2 peak and PbTe showed some structure at the E_3 peak. A detailed curve of part of the E_2 maximum for PbS both at room temperature and 77°K is shown in Fig. 3. We have not been able to interpret this fine structure. It was extremely difficult to make good estimates of temperature coefficients of the maxima owing to the broad nature of the peaks. The error in such estimates is consequently rather large. All measurements of the E_1 , E_2 , and E_3 maxima pointed however to a zero or small positive temperature coefficient, a surprising result in view of the large positive coefficient of the direct optical gap, and the negative coefficient observed in the majority of diamond and zinc-blende materials. Detailed curves of the E_3 peak in PbTe are also shown

in Fig. 3. A value of $dE_3/dT = (+1.0 \pm 1.5) \times 10^{-4} \text{ eV } (^\circ\text{C})^{-1}$ is obtained for this peak.

The room-temperature reflectivity of As, Sb, and Bi is shown in Figs. 4 to 6; also included in these curves are the values at 77°K for energies less than 6 eV. The results for Bi have been extended further to lower energies, and show the large drop in reflection coefficient in the infrared, due to the plasma edge. The reflectivity of Sb and Bi at low energies undergoes a sharp rise on cooling to 77°K. This effect, which does not seem to be due to experimental troubles is at present unexplained. The cleaved surfaces of both materials were extremely stable, and showed no signs of oxidation after being kept for periods of months in air. It is in fact the curve for As that should be treated with caution, because although the sample was placed in vacuum directly after cleaving, it is oxidized rapidly on subsequent exposure to the atmosphere.

The thin-film transmission measurements at room temperature and 77°K for the three lead salts and SnTe

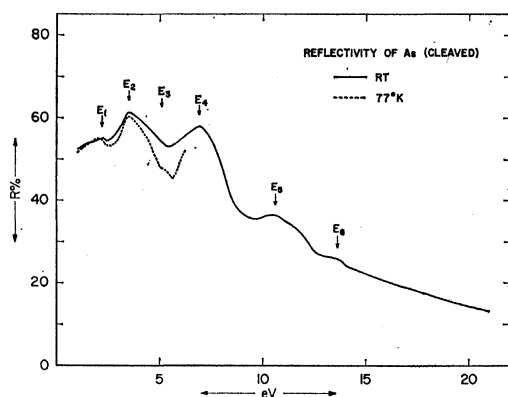


FIG. 4. Room-temperature reflectivity of As, and region below 6 eV at 77°K.

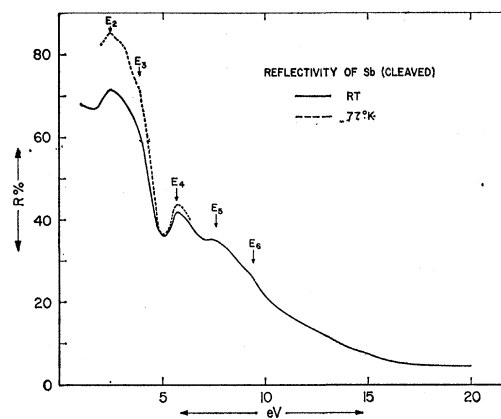


FIG. 5. Room-temperature reflectivity of Sb, and region below 6 eV at 77°K.

are shown in Figs. 7 to 10. The absorption coefficients calculated from the reflectivity using the Kramers-Kronig relations (see Sec. IV) are also shown in these figures. The transmission results at room temperature have been normalized to agree in magnitude with the reflectivity results at the position of maximum absorption. Using the results in Figs. 7 to 10 together with the measured reflectivity and the values of n and k taken from the Kramers-Kronig results, it is possible to calculate the film thickness from the expression $I = I_0(1-R)^2(1+k^2/n^2) \exp(-\alpha d)$, which applies in the region of highest absorption for these materials. (This expression only applies when the medium both sides of the film is the same, however, since the refractive index of the alkali halides is small, the correction due to the substrate is negligible.) Using this procedure the following thicknesses are obtained for the films of Figs. 7 to 10: PbS 340 Å, PbSe 250 Å, PbTe 280 Å, and SnTe 300 Å, in excellent agreement with the thicknesses measured directly using the Tolansky method.

The transmission results given here show a consistent deviation at low energies from the absorption curves obtained from the Kramers-Kronig analysis. This deviation is due to the effect of multiple internal reflections in a region where the films are relatively transparent. We have made no attempt to compute this effect in detail, but a rough calculation shows that the difference can be completely accounted for by the presence of these reflections.

The E_1 absorption peak of PbSe is seen to sharpen considerably at low temperature. This peak in the other materials does not change appreciably on cooling. This behavior was also noted in reflectivity, where it was observed that the PbSe E_1 peak became much sharper at 77°K, but PbS, PbTe, and SnTe did not change.

It should be noted that the absorption curves reported here are essentially in good agreement with the early results of Gibson.¹⁰ There is no evidence however for the long low-energy absorption plateau reported by

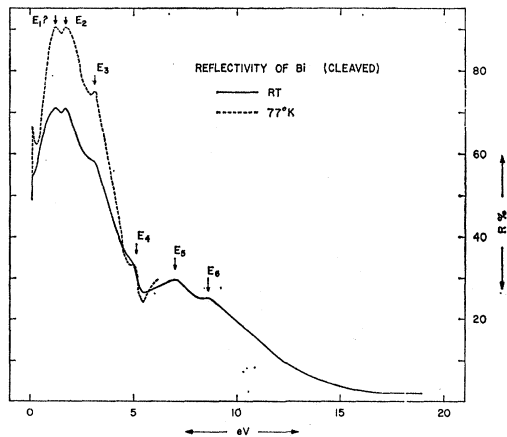


FIG. 6. Room-temperature reflectivity of Bi, and region below 6 eV at 77°K.

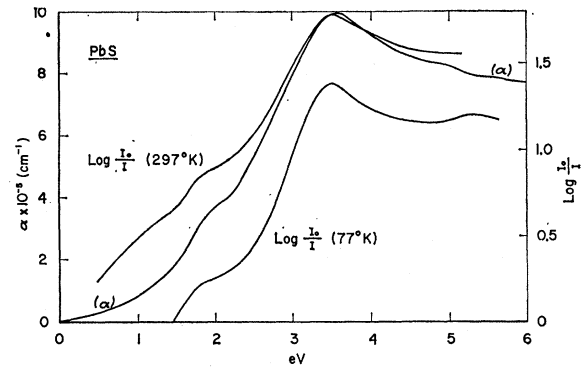


FIG. 7. Transmission of PbS at RT and 77°K, with room-temperature absorption coefficient (α) calculated from the reflectivity.

Scanlon¹³ which we believe is due to the presence of pinholes in the samples or scattered light in the monochromator.

The collected results of both reflection and transmission for all the materials studied are given in Table I. The energies of the E_1 , E_2 , and E_3 maxima have been obtained by three methods: (1) direct from the reflectivity peaks, (2) from the maxima in absorption coefficient (α) computed from the reflectivity data using the Kramers-Kronig relation, and (3) from the maxima in the thin-film transmission curves. In the case of the E_2 peak, figures are also given for maxima in the function $\epsilon_2 E^2$ (where $\epsilon_2 = 2nk$, the imaginary part of the dielectric constant). This function is proportional to the joint density of states if the matrix element of \mathbf{p} determining the E_2 transition remains constant. Considerable differences exist between the maximum values obtained by the various methods, in particular between the reflectivity peaks and the maxima in the density of states. This is a consequence of the broad nature of the peaks in all these materials, in contrast to the relatively sharp structure associated with diamond and zincblende substances. (In these last materials the shift between the peaks determined by reflection, transmission and from $\epsilon_2 E^2$ is less than 0.1 eV.)

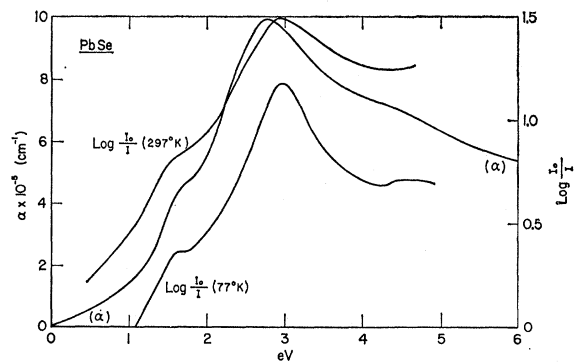


FIG. 8. Transmission of PbSe at RT and 77°K with room-temperature absorption coefficient (α) calculated from the reflectivity.

TABLE I. Collected results.

			PbS	PbSe	PbTe	SnTe	SeTe	As	Sb	Bi
E_0	Onset of indirect transitions (Gibson and Scanlon)	RT 77°K	0.37 0.30	0.26 0.18	0.29 0.21					
E_1	From reflectivity Peak in α from Kramers-Kronig From thin-film transmission	RT	1.83	1.54	1.24			2.2		1.2
		RT	1.95	1.55	1.25	0.9				
		RT	1.88	1.59	1.26	0.97				
		77°K	1.85	1.59	1.24					
E_2	From reflectivity Peak in α from Kramers-Kronig From thin-film transmission	RT	3.67	3.12	2.45	2.07	1.98	3.5	2.5	1.7
		RT	3.54	2.75	2.30	2.00			2.5	
		RT	3.52	2.98	2.20	1.96				
		77°K	3.49	2.95	2.18	1.95				
E_3	Maximum in nkE^2 From reflectivity Peak in α from Kramers-Kronig From thin-film transmission	RT	3.20	2.52	1.98	1.82			2.0	
		RT	5.3	4.5	3.5	3.2	3.2	5.1	3.9	3.1
		RT	5.0	4.4	3.5	3.1				3.9
		RT	5.23 ^a	4.65	3.36	3.06				
E_4	From reflectivity	RT	8.1	7.1	6.3	6.1	5.4	6.9	5.7	5.0
E_5	From reflectivity	RT	9.8	9.1	7.8	7.4	6.2	10.6	7.6	7.0
E_6	From reflectivity	RT	13.9	12.5	11.2	9.1	7.8	13.6	9.4	8.6

^a Substrate absorbing strongly.

The thin-film transmission results allow an accurate estimate to be made of the temperature coefficients of the three low-energy peaks in the lead salts and SnTe. The figures given in Table I confirm the trends indicated by the reflectivity curves, and reveal a small positive coefficient for all three peaks. A possible explanation for these low coefficients is put forward in Sec. V.

IV. KRAMERS-KRONIG ANALYSIS

A. Procedure

The real and imaginary parts of the refractive index n and k can be obtained¹ from the reflectivity spectrum at normal incidence $R(E)$ (E =photon energy) by calculating the integral

$$\theta(E_0) = \frac{1}{2\pi} \int_0^\infty \frac{d \ln R(E)}{dE} \ln \left| \frac{E+E_0}{E-E_0} \right| dE. \quad (1)$$

n and k are then given as the solution of the equation:

$$(n-ik-1)/(n-ik+1) = R^{1/2} e^{i\theta}. \quad (2)$$

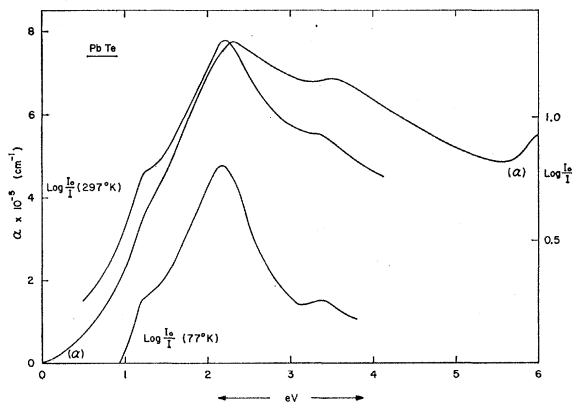


FIG. 9. Transmission of PbTe at RT and 77°K with room-temperature absorption coefficient (α) calculated from the reflectivity.

Equation (1) is readily obtained by substituting Eq. (2) into the conventional Kramers-Kronig relations.

The integrand in Eq. (1) is singular for $E=E_0$ and the integral is to be interpreted as the Cauchy principal value. In order to handle Eq. (1) with a computer, it is convenient to transform it so as to remove this singularity. This can be easily accomplished by adding to the integrand²⁰:

$$-\frac{d \ln R(E_0)}{dE} \ln \left| \frac{E+E_0}{E-E_0} \right| = 0.$$

Integrating by parts we then obtain

$$\theta(E_0) = \frac{E_0}{\pi} \int_0^\infty \frac{\ln R(E) - \ln R(E_0)}{E^2 - E_0^2} dE. \quad (3)$$

The transformation from Eq. (1) to Eq. (3) is justifiable for all physically meaningful reflection spectra. The integrand in Eq. (3) is finite for $E \rightarrow E_0$ provided the reflectivity spectrum does not have an infinite slope at E_0 . Such infinite slopes are never encountered experimentally.

Since the spectral region of the reflectivity measurements is always bounded ($E < 25$ eV in our measurements), it becomes necessary to extrapolate $R(E)$ to infinite energies in order to compute n and k . Most of the optically strong transitions occur within the region of our measurements, the oscillator strengths beyond 25 eV being extremely small as evidenced by the low reflectivity. Hence the simplest extrapolation can be made by lumping all oscillator strengths into a single frequency and assuming that the absorption above 25 eV is practically zero while the dispersion is given by the single oscillator dispersion. One then obtains

$$R \cong CE^{-4}. \quad (4)$$

²⁰ We are grateful to Dr. R. W. Klopfenstein for suggesting this transformation.

In Ref. 1 the exponent of Eq. (4) was taken to be an adjustable parameter and adjusted *ad hoc* until the best agreement between calculated and experimental absorption coefficients at low temperatures was obtained. We have simply taken an exponent equal to -4 and obtained good agreement with transmission data.

In order to process the data with a computer, the integral in Eq. (1) is decomposed into an integral with the experimental $R(E)$ between 0 and 25 eV and an integral with $R=CE^{-4}$ from 25 eV to infinity (C is calculated so as to have the reflectivity continuous at 25 eV). In order to evaluate the first integral, the spectrum is divided into 0.1 eV intervals and a parabola is fitted to each three consecutive points. The integral for each parabolic segment is calculated in closed form as a function of the coefficients of the parabola and the contribution from each segment is added up by the computer. The integral from 25 eV to infinity can be transformed into

$$\int_{25}^{\infty} \frac{\ln R(E) - \ln R(E_0)}{E^2 - E_0^2} dE = \frac{1}{2E_0} [\ln C - \ln R(E_0)] \ln \frac{25 + E_0}{25 - E_0} - \frac{4}{E_0} \sum_{r=0}^{\infty} \left(\frac{E_0}{25}\right)^{2r+1} [1 + (2r+1) \ln 25]. \quad (5)$$

Equation (5) is summed with the computer.

B. Results

We have only applied the Kramers-Kronig analysis to the room-temperature reflection data, since the low-temperature data do not extend into the vacuum ultraviolet region. This analysis has been made for the reflection data in the lead salts, SnTe, and antimony cleaved perpendicular to the hexagonal (optical) axis. The optical constants obtained for antimony refer to propagation along this axis. Figures 11–15 show the optical constants n and k obtained for PbS, PbSe, PbTe, SnTe, and Sb, respectively.

We have also plotted in these figures the imaginary part of $-1/\epsilon$ (ϵ is the dielectric constant) which, as we shall discuss in the next section, is proportional to the characteristic energy loss for transmission of electron beams through thin films. For the sake of completeness we have plotted in Fig. 16 the real and the imaginary part of the dielectric constant (ϵ_1 and ϵ_2 , respectively) for PbTe at room temperature, as calculated from the optical constants of Fig. 13. Figure 17 shows the function $\epsilon_2 E^2$, which is roughly proportional to the combined density of states for the optical transitions, for PbTe and for germanium.⁵

V. DISCUSSION

The energies of the reflectivity peaks of the lead salts, SnTe and GeTe are plotted in Fig. 18 as a function of lattice parameter. Values for E_0 have been taken

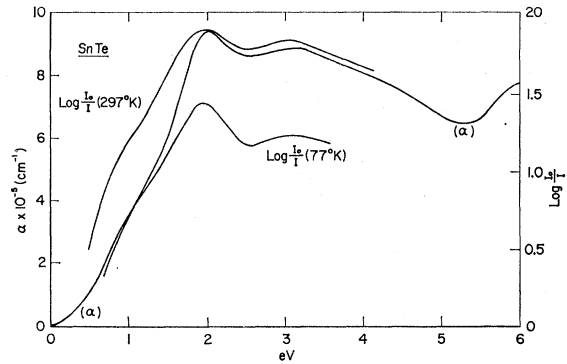


FIG. 10. Transmission of SnTe at RT and 77°K with room-temperature absorption coefficient (α) calculated from the reflectivity.

from Scanlon's absorption curves. The corresponding results for As, Sb, and Bi are shown in Fig. 19. These figures, and the similarities between all the reflectivity curves, make it reasonable to assume that corresponding peaks are caused by the same mechanism in each material. This is certainly true for the E_1 - E_6 peaks of the three lead salts.

The most striking feature of Fig. 18 is the decrease of all gaps (E_1 - E_6) when lead is substituted by an atom of the same column and smaller atomic number (Sn, Ge). In diamond and zinc-blende-type materials, gaps involving an s -like conduction-band state always decrease with increasing atomic number (the smallest direct gap of ZnS is larger than that of ZnO but this seems to be the only exception to the rule). This is to be expected since the energy of states with a nonvanishing wave function at the core decreases very rapidly with increasing atomic number.³⁰ Gaps between p - or d -like states

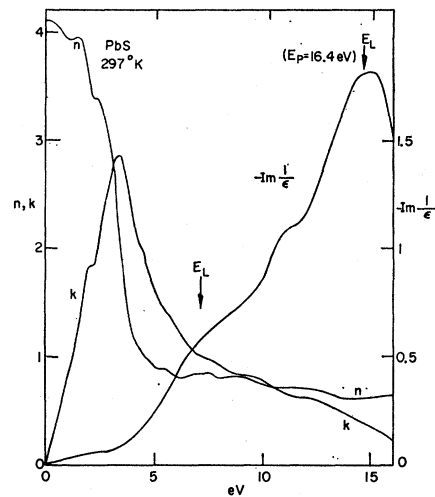


FIG. 11. Room-temperature Kramers-Kronig analysis and energy-loss function for PbS.

³⁰ F. Herman and W. S. Skillman, *Proceedings of the International Conference on Semiconductor Physics, Prague, 1960* (Czechoslovakian Academy of Sciences, Prague 1961), p. 20.

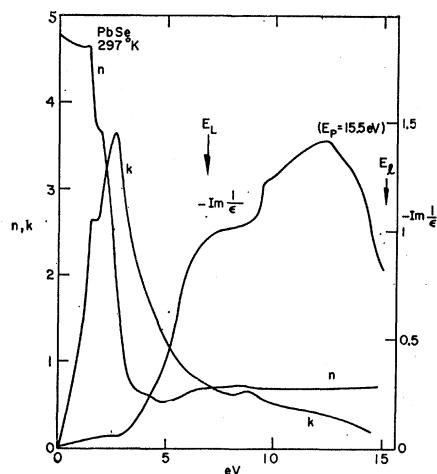


FIG. 12. Room-temperature Kramers-Kronig analysis and energy-loss function for PbSe.

do not change much when the atomic number of one of the components is changed. These gaps sometimes increase when the atomic numbers are increased (e.g., the $\Gamma_{15}-\Gamma_{15}$ gap GaP-InP, CdS-ZnS-ZnSe, CdTe-ZnTe³¹). As we shall see later, the E_0 , E_1 , E_2 , and E_3 gaps are energy differences between predominantly p -type states and hence a decrease in these gaps when replacing lead by tin or germanium is not surprising. The E_4 , E_5 states are interpreted in the following discussion as gaps between an s -like valence-band state and a p -like conduction band. With increasing atomic number, the

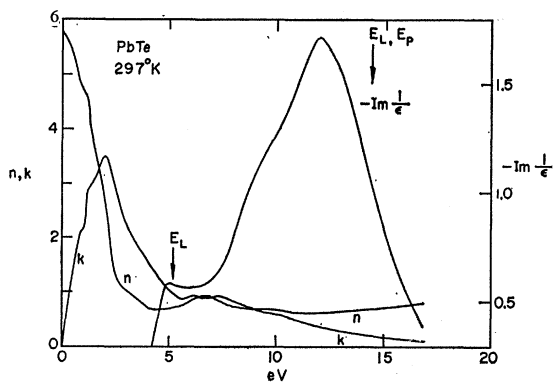


FIG. 13. Room-temperature Kramers-Kronig analysis and energy-loss function for PbTe.

energy of the s -like state decreases faster than that of the p -like state and hence an increase in the gap is to be expected. The nature of the conduction band associated with the E_6 state is not clear and hence such a discussion cannot be given for this state.

PbS formed the subject of an early band structure calculation.³² This analysis showed that the energy bands were not simple paraboloids about the origin

³¹ M. Cardona, Phys. Chem. Solids (to be published).

³² D. G. Bell, D. M. Hum, L. Pincherle, D. W. Sciamia, and P. M. Woodward, Proc. Roy. Soc. (London) **A217**, 71 (1953).

of \mathbf{k} space, but contained various maxima and minima at nonzero \mathbf{k} values. The calculations indicated however that the minimum separation between valence and conduction bands occurred along the $[110]$ direction, and not at the center of the Brillouin zone. We have based our interpretation of the band structure of the materials here, on the recent APW calculation on PbTe carried out by Johnson *et al.*⁹ The essential results of this calculation are shown in Figs. 20 and 21. Figure 20 shows the E versus \mathbf{k} curves for the three symmetry directions in \mathbf{k} space: $[111]$, $[110]$, and $[100]$, together with an indication of the atomic precedence of the vari-

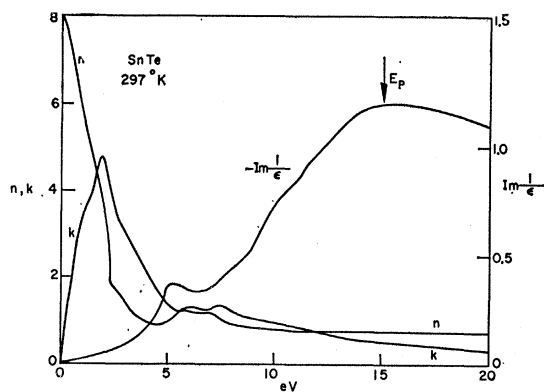


FIG. 14. Room-temperature Kramers-Kronig analysis and energy-loss function for SnTe.

ous states at $\mathbf{k}=0$. Figure 21 shows the preliminary results in one direction $[111]$ of the same calculation modified to include the rather large spin-orbit interaction (the atomic spin-orbit splitting in Pb is of the order of 1 eV). (See note added in proof.) It has been pointed out³³ that, in the zinc-blende-type materials, structure in the optical spectra arises from transitions between states which are degenerate in the empty lattice; only these states yield large enough matrix elements of \mathbf{p} . This rule can be easily justified if there is no appreciable mixing between the various empty

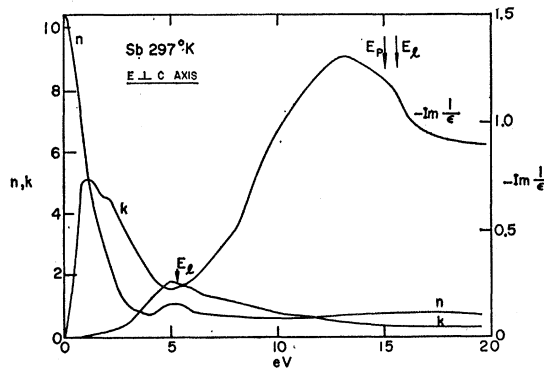


FIG. 15. Room-temperature Kramers-Kronig analysis and energy-loss function for Sb.

³³ J. C. Phillips (private communication).

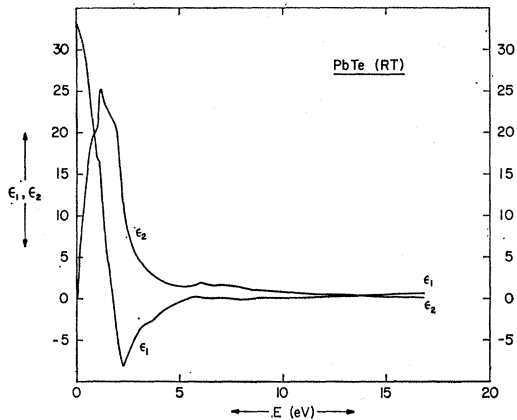


FIG. 16. Real and imaginary parts of the dielectric constant ϵ_1 and ϵ_2 for PbTe (room temperature).

lattice states belonging to different energies. In the lead salts these states are heavily mixed: the $\mathbf{k}=0$ gap (see Fig. 20) is formed from states which belong to two different empty lattice eigenvalues. The next $\mathbf{k}=0$ conduction band (Γ_{25}'), however, belongs to the same empty lattice eigenvalue as the Γ_{15} valence band.

This rule can still be used to exclude optical transitions from the lowest valence band (Γ_1 at $\mathbf{k}=0$) to any conduction band.

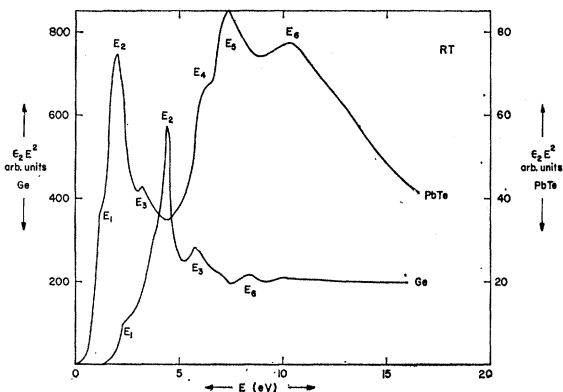


FIG. 17. Combined density of states function $\epsilon_2 E^2$ (in arbitrary units) for germanium and PbTe, as obtained from the Kramers-Kronig analysis (room temperature).

E₀ Transitions

The calculations shown in Fig. 21 indicate that the minimum band separation for PbTe occurs in the $[111]$ direction in agreement with the experimental evidence referred to in Sec. I. The calculation also indicates that the valence band between Γ and L is rather flat, with a maximum near the midpoint of the zone. The experiments, however, indicate that the top of the valence band is at the L point.¹⁶ We can attribute this to inaccuracies in the band calculations: a simple distortion of the Λ_6 band in Fig. 21 brings the maximum to the L point. The smallest allowed direct-energy gap (E_0)

corresponds to $L_6^+ - (L_4^-, L_5^-)$ (the L_4 and L_5 states are degenerate due to time-reversal symmetry) and, if the band calculation is correct, should correspond to the direct absorption edge of the material.¹³ The indirect edge could be due to optical phonon absorption at the same states or to transitions from valence-band states higher than L_6^+ , which may exist according to Fig. 21.

The direct absorption edge for PbS and PbSe looks quantitatively the same (only shifted in energy) as in PbTe.¹³ Also the "anomalous" temperature coefficient of this edge is the same in the three materials, hence it

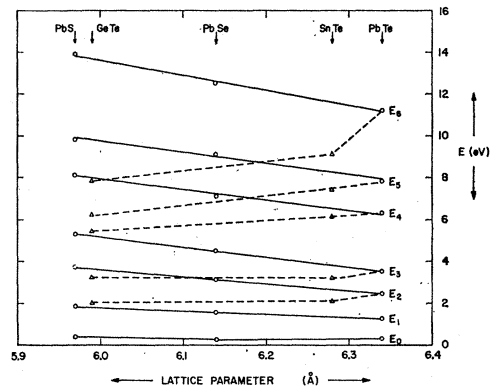


FIG. 18. Reflectivity-peak energies plotted against lattice parameter for PbS, PbSe, PbTe, SnTe, and GeTe. (E_0 values taken from Scanlon's absorption results.)

looks very much as if the direct gaps of the three materials were due to the same type of transitions at the L point. The work of Palik and Mitchell¹⁹ suggests that the valence- and conduction-band states which produce the E_0 edge are nondegenerate in PbS. This would rule out the possibility of transitions at $\mathbf{k}=0$, since the highest valence band at this point will most likely also be the Γ_8^- for PbS and hence will be degenerate. However, the interband magnetoabsorption measurements¹⁹ seem to indicate that the states producing the E_0 gap have spherical energy surfaces. While this is not totally impossible for an L gap, it is sur-

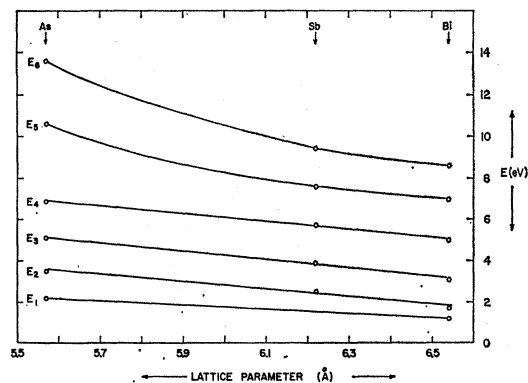


FIG. 19. Energies of reflectivity peaks plotted against lattice parameter for As, Sb, and Bi.

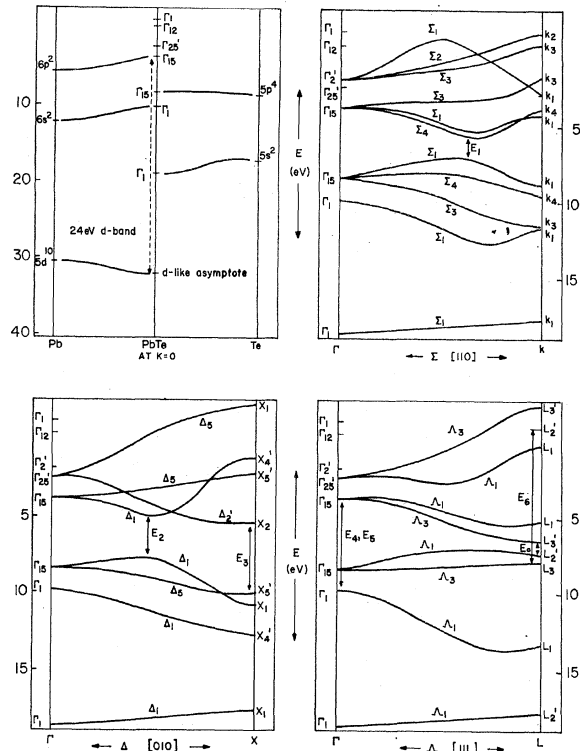


FIG. 20. Results of APW energy band calculation for PbTe obtained by Johnson *et al.*, excluding spin-orbit interaction.

prising; one would expect some anisotropy if the constant energy surfaces are not centered at $\mathbf{k}=0$. Also piezoresistance measurements in¹⁸ PbSe indicate that the lowest conduction-band minimum and the highest valence-band maximum are isotropic; these states could occur at $\mathbf{k}=0$ but be of the same parity so that optical transitions between them are forbidden. We think this possibility is rather improbable.

Figure 18 shows that E_0 for PbSe occurs at slightly lower energy than for the other two lead salts. This could be produced by the high spin-orbit mixing of the conduction- and valence-band states involved in the E_0 transitions.

From the above proposed band scheme, it is possible to suggest a qualitative explanation for the large positive temperature coefficient associated with the optical gaps in the lead salts. The temperature coefficient of an energy gap can be written as the sum of two terms:

$$\left(\frac{\partial E}{\partial T}\right)_P = \left(\frac{\partial E}{\partial V}\right)_V + \frac{1}{V} \left(\frac{\partial V}{\partial T}\right)_P V \left(\frac{\partial P}{\partial V}\right)_T \left(\frac{\partial E}{\partial P}\right)_T, \quad (6)$$

where $(1/V)(\partial V/\partial T)_P$ = volume expansion coefficient and $(V(\partial P/\partial V))^{-1}$ = the volume compressibility. The first term in Eq. (6) is due to electron-phonon interaction, and in diamond and zinc-blende materials is negative and equal to approximately -2×10^{-4} eV/°C. The second term is due to the dilation of the lattice. In

diamond and zinc-blende semiconductors this term is also generally negative, consequently, one obtains a total coefficient that is of the order of -4×10^{-4} eV/°C for most of the interband transitions. Paul has shown, however,³⁴ that for PbS and PbSe, and possibly also PbTe, the second term is positive and equal to $+2 \times 10^{-4}$ eV/°C. This means that for the E_0 gap the electron-phonon interaction must also give a positive contribution. This can, in principle, happen when a band extremum causing the transition is not the absolute extremum of the band. If, for example, there exists a valence-band extremum at a slightly higher energy, then the perturbation caused by this band can shift the lower band downwards as the temperature is raised and lead to a positive electron-phonon contribution. It is exactly this type of valence-band structure that we propose for the lead salts. The L_6^- valence-band state, acting as an intermediate state for the phonon interaction, could lower the L_6^+ state and thus give a positive temperature coefficient for E_0 . (See note added in proof.)

E₁ Transitions

The second minimum band separation in PbTe lies in the [110] direction (Σ_1 - Σ_4 transitions) according to Fig. 20, and the E_1 peak is assigned to this point. The [110] conduction band probably has at this point a saddle-point type of structure since the energy difference increases when moving away from E_1 in the [110] direction and decreases when moving towards the [111] points. This behavior has an analog in the zinc-blende materials, where both main near ultraviolet reflectivity maxima (Λ_3 - Λ_1 and X_5 - X_1) are due to transitions at

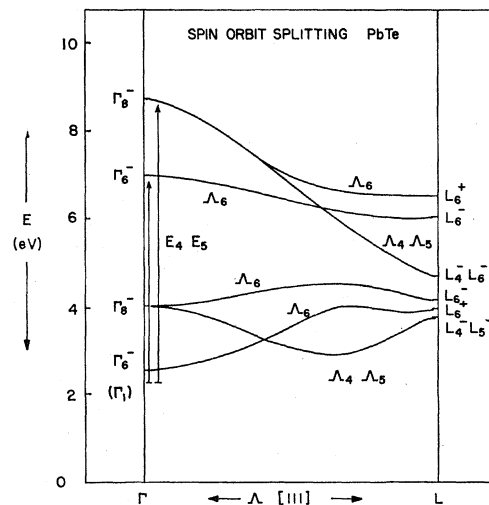


FIG. 21. Preliminary results of energy-band calculation by Johnson *et al.* for PbTe in [111] direction, including spin-orbit interaction.

³⁴ W. Paul, M. De Meis, and L. X. Finogold, *Proceedings of the International Conference on the Physics of Semiconductors, Exeter, 1962* (The Institute of Physics and the Physical Society, London, 1962), p. 712.

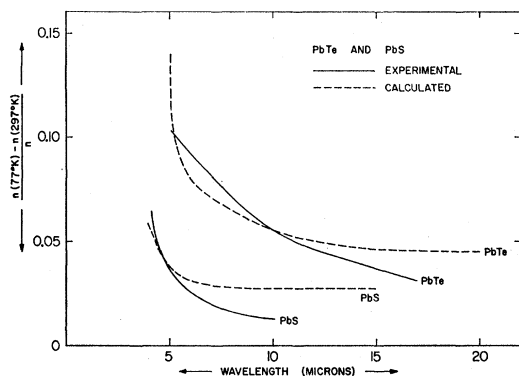


FIG. 22. Experimental and calculated variation of the refractive index with temperature for PbS and PbTe.

an M_1 saddle point.³⁶ The calculated energy of the E_1 transition in PbTe (1.4 eV) agrees well with the experimental value of 1.24 eV. The shape of the E_1 edge (see Figs. 16 and 17) also seems to suggest transitions at an M_1 -type saddle point.

The E_1 gap shows a very small temperature dependence (see Table I), about $+10^{-4}$ eV \times ($^{\circ}$ C) $^{-1}$ for PbTe and PbS and smaller than our experimental error [0.5×10^{-4} eV \times ($^{\circ}$ C) $^{-1}$] for PbSe.

E_2 and E_3 Transitions

The absolute maximum in reflectivity in zinc-blende materials is caused by two saddle-point singularities (at the X and Σ points) very close in energy.³⁵ These saddle points are of the M_1 (X) and M_2 (Σ) type: the rise in density of states with energy due to M_1 combines with the fall due to M_2 and gives a very sharp peak. The highest (E_2) peak shown in Figs. 8 to 17 seems to indicate a similar type of singularity for the materials under consideration here. An examination of Fig. 20 shows that the E_2 peak could be due partly to the saddle point associated with Δ_1 - Δ_1 transitions (in the $[100]$ direction, like the X transitions causing E_2 for zinc-blende materials). According to the calculations, these transitions occur at 2.8 eV, reasonably close to the values listed in Table I for the various E_2 peaks in PbTe (these peaks occur at wavelengths somewhat smaller than 2.8 eV; however, it is expected that spin-orbit interaction will decrease the gaps shown in Fig. 20). The other saddle-point singularity postulated in order to explain the E_2 peak cannot be easily identified due to the incomplete nature of the calculations depicted in Fig. 20. One possibility would be the Δ_1 - Δ_2' transitions, however, the singularity could also occur, like in zinc blende, in the Σ direction. We have also tentatively assigned the E_3 peak to X_5 - X_2 transitions. The Γ_{15} - Γ_{15} transitions, which give a gap close to E_3 , are forbidden by parity.

³⁵ D. Brust, J. C. Phillips, and F. Bassani, Phys. Rev. Letters **9**, 94 (1962).

The E_2 gap has a small positive temperature coefficient of about 10^{-4} eV \times ($^{\circ}$ C) $^{-1}$ for the lead salts and SnTe. A similar behavior is observed for the E_3 gap in PbTe and SnTe; the negative coefficient observed for PbS is believed to be spurious due to the incipient absorption of the NaCl substrate.

The electronic contribution to the long-wavelength intrinsic refractive index of the lead salts is mostly produced by the E_2 absorption. The large temperature coefficient of the refractive index reported by Avery³⁶ for PbS [$dn/dT = -6\times 10^{-4}$ ($^{\circ}$ C) $^{-1}$] cannot be due to the shift of the E_2 edge with temperature and must be attributed to the variation with temperature of the small contribution of E_0 to the dispersion. This contribution can be estimated to be, under the assumption of perfect parabolicity for the bands giving the E_0 gap³⁷:

$$4\pi\chi_{E_0}(E) = Am^{*3/2}E^{-2}[2E_0^{1/2} - (E_0 - E)^{1/2} - (E_0 + E)^{1/2}], \text{ for } E \leq E_0. \quad (7)$$

The constant A , which is proportional to a square matrix element for the E_0 transitions, can be determined from recent dispersion data obtained by Zemel.³⁸ The contribution of E_0 to the zero-frequency dielectric constant is about 5 for PbTe and PbS. This value is much larger than the contribution of the fundamental direct-absorption edge E_0 to the dielectric constant of germanium and zinc-blende-type materials due to the fact that E_0 in these materials occurs at $k=0$ while it occurs at the L point in the lead salts. Thus the density of states for the transitions is larger in the latter than in the former materials. Figure 22 shows the temperature dependence of n calculated from Eq. (7) and the known temperature dependence of E_0 .¹³ m^* is assumed temperature-independent since the longitudinal component of it is not determined by E_0 and the transverse component is only affected by the thermal expansion contribution to dE_0/dT . A is also assumed to be temperature-independent. We have measured the temperature dependence of n by measuring the shift with temperature of the interference fringes produced in the infrared by thick epitaxial films of PbS and PbTe (see Sec. II). The results, also shown in Fig. 22, are in good qualitative agreement with the calculations based on Eq. (7). The temperature dependence remanent at long wavelengths may be due to some free-carrier contribution to the dispersion.

E_4 and E_5 Transitions

Figure 17 emphasizes the similarity between the band structures of the lead salts and germanium. The only striking difference is the presence of the two extra peaks E_4 and E_5 in the lead salts. One is thus tempted to attribute these peaks to the two extra electrons per unit

³⁶ D. G. Avery, Proc. Phys. Soc. (London) **B67**, 2 (1954).

³⁷ L. I. Korovin, Fiz. Tverd. Tela **1**, 1311 (1959) [English transl.: Soviet Phys.—Solid State **1**, 1202 (1959)].

³⁸ J. Zemel (to be published).

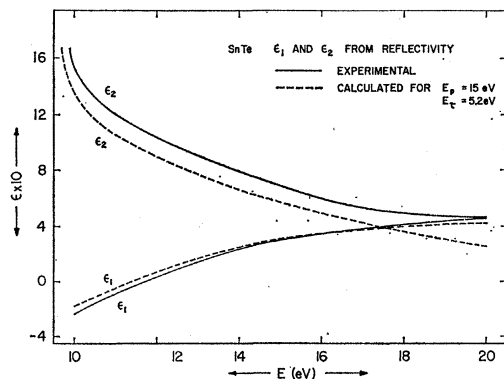


FIG. 23. Experimental and calculated curves of ϵ_1 and ϵ_2 for SnTe at high energies ($E_p=15$ eV, $E_\tau=5.2$ eV).

cell that the lead salts have, compared with germanium. These two electrons occupy the second lowest Γ_1 band (see Fig. 20). We have tentatively assigned the E_4 and E_5 peaks to transitions from this Γ_1 level to the spin-orbit split Γ_{15} conduction band. The E_4 - E_5 splitting would thus correspond to the spin-orbit splitting of the Γ_{15} states. Figure 21 shows that this splitting is 1.7 eV, in good agreement with the experimental E_4 - E_5 splitting in PbTe. Furthermore from Fig. 20 it is seen that the conduction band at $\mathbf{k}=0$ is formed mostly from the 6 p electrons of lead. One might therefore expect the E_4 - E_5 splitting to remain constant in the three lead salts, and to decrease for SnTe and GeTe with decreasing atomic number of the Group IV atom; in Fig. 17, it is seen that this behavior does take place.

E_6 Transitions

The E_6 shown for germanium in Fig. 17 seems to be the peak assigned by Phillips³⁹ to L_1 - L_2' transitions. According to Fig. 20, the L_3 - L_2' gap is 9 eV in PbTe and thus the experimentally observed E_6 peak (11 eV) could be caused by these transitions. L_3 and L_2' are degenerate in the empty lattice. Other possibilities can be suggested by inspection of Fig. 20 (such as lowest Γ_1 - Γ_{15}) but most of them correspond to transitions between states which belong to different empty lattice eigenvalues.

d Bands

Figure 1 shows the presence of a rise in reflectivity at high energies (above 15 eV). The rise is observed in the three lead salts, but not for SnTe and GeTe. This effect is clearly due to transitions from filled d bands to the conduction band. In the lead salts the d bands arise from the atomic d bands of lead, and are located about 24 eV below the conduction band. In SnTe and GeTe the d bands lie much deeper, and should not be observed over the energy range studied here. The rise in reflectivity at high energies due to d bands has already been

observed in a number of zinc-blende semiconductors^{6,7} and the effect in the lead salts is completely analogous. No d -electrons effect is seen in As, Sb, and Bi (Figs. 5-7) due to the depth of the d electron in these materials (~ 50 eV).

Plasma Region

In the region where the oscillator strengths for the optical transitions are mostly exhausted, the dielectric constant can be represented by the classical Drude formula⁴⁰:

$$\epsilon(E) \approx 1 - \omega_{pv}^2 (E/\hbar + i/\tau_v)^{-2}, \quad (8)$$

where τ_v is an average collision time, $\omega_{pv}^2 = 4\pi e^2 N_v/m$ is the plasma frequency of the valence electrons, N_v is their density and m the free-electron mass. Due to the E_4 and E_5 transitions, the region of applicability of Eq. (8) is smaller in the materials under consideration here than in germanium and in the III-V compounds. We have chosen SnTe for comparison with Eq. (8) since the E_4 and E_5 transitions occur in this material at rather low energies and the d -electron transitions at high energies. Figure 23 shows the real and imaginary parts of the dielectric constant of SnTe obtained from the Kramers-Kronig analysis of the reflection data (full line) and the best experimental fit (broken line) obtained with Eq. (8). The only adjustable parameter is $E_\tau = \hbar/\tau_v$, which is set equal to 5.2 eV. The plasma frequency ω_{pv} is calculated by taking $N_v = 5$ electrons/atom. The scattering time τ_v is equal to 1.3×10^{-16} sec, very close to the values obtained for zinc-blende-type materials⁴⁰ (1.4×10^{-16} - 1.8×10^{-16} sec).

In Figs. 11 to 15 we have plotted the characteristic energy function $-\text{Im}(1/\epsilon)$ calculated from the Kramers-Kronig analysis of the reflection, for the lead salts, SnTe and Sb. A quantitative agreement between these results and the results obtained by means of electron beams⁴¹ does not exist, probably due to the imperfect nature of the films used in the electron beams experiments and also to the inaccuracy of the data obtained from the Kramers-Kronig analysis (a large peak in $-\text{Im}(1/\epsilon)$ is obtained from the analysis of the very small, inaccurate reflection in the plasma region). However, the structure observed in the beams experiments (peaks marked E_L in our figures) roughly corresponds to structure obtained in the Kramers-Kronig analysis. The main peak in the energy-loss function occurs approximately at the plasma energy E_p . The secondary peak between 5 and 8 eV seems due to the E_4 and E_5 transitions. No electron beams data are available for SnTe.

CONCLUSIONS

The reflection spectra of PbS, PbSe, PbTe, SnTe, GeTe, As, Sb, and Bi have been measured under normal

³⁹ J. C. Phillips, Phys. Rev. **133**, A452 (1964).

⁴⁰ H. R. Philipp and H. Ehrenreich, Phys. Rev. **129**, 1550 (1963).

⁴¹ L. B. Leder, Phys. Rev. **103**, 1721 (1956).

incidence in the region between 0.5 and 25 eV. A striking similarity between these spectra has been found and some analogy between these and the spectra of germanium and zinc-blende-type materials has been suggested. Six reflection peaks have been found in all these materials. The energy of these peaks increases through the sequence PbTe-PbSe-PbS but, unexpectedly, decreases through PbTe-SnTe-GeTe. The reflection results have been analyzed by the Kramers-Kronig method and the optical constants determined for PbS, PbSe, PbTe, SnTe, and Sb along the optical axis.

The absorption constants obtained have been compared with transmission measurements made on thin epitaxial films of PbS, PbSe, PbTe, and SnTe. The agreement has been shown to be excellent. An attempt has been made to interpret these peaks in terms of transitions at Van Hove's singularities in the energy difference between bands at high symmetry points (X, L, Γ) and lines (Δ, Σ, Λ). The temperature shift of the E_1 , E_2 , and E_3 peaks has been measured and found to be about $+10^{-4} \text{ eV} \times (^\circ\text{C})^{-1}$ for almost all materials under consideration. This shift has been compared with the measured temperature variation of the refractive index and it has been concluded that this variation is mostly due to the large shift of the fundamental edge (E_0) with temperature.

The effect of the d electrons of lead on the optical spectra has been observed in the lead compounds. In all other materials under consideration, this effect lies beyond our experimental photon energy range.

The quasifree electron region (plasma region) of SnTe has been studied in detail. It has been shown that the phenomenological scattering time required to fit the optical constants with the Drude formula is 1.3×10^{-16} sec. The characteristic energy loss function $-\text{Im}(1/\epsilon)$ has been obtained from the Kramers-Kronig

analysis for the lead salts, SnTe, and antimony. The results are in qualitative agreement with electron transmission data. The structure which appears in these data between 5 and 8 eV has been interpreted in terms of interband transitions.

Note added in proof. It has been recently shown^{42,43} that relativistic effects other than spin-orbit interaction can alter significantly the band structure of PbTe and similar materials. The labeling of the energy eigenvalues at the L point, calculated taking these effects into account, differs from Fig. 2: the minimum energy gap is $(L_4^+, L_5^+) \rightarrow L_6^-$, allowed for optical transitions. While no detailed calculations at points other than L have been published, it is easy to estimate that the $\Delta_1 - \Delta_1$ and $X_{5'} - X_2$ gaps are decreased by the relativistic effects⁴³ thus improving the agreement with the experimental E_2 and E_3 gaps. These effects should also lower the Γ_1 valence band state (s state of the lead) by about 7 eV,⁴³ thus making the interpretation of the E_4 and E_5 peaks questionable. A final assignment of the optical structure will have to wait until complete relativistic energy band calculations become available.

ACKNOWLEDGMENTS

We would like to thank Oleh Tkál for performing many of the optical measurements and Tom Stiller for the programming and processing of the optical data. Thanks are also due to Dr. R. W. Klopfenstein for help in the Kramers-Kronig programming and Dr. J. N. Zemel and Dr. G. W. Pratt for sending us their data prior to publication. We should also like to thank Dr. W. Lawson (R.R.E. Malvern, England) for providing single-crystal samples of the three lead salts.

⁴² L. E. Johnson, J. B. Conklin, and G. W. Pratt, Jr., *Phys. Rev. Letters* **11**, 538 (1963).

⁴³ F. Herman, C. D. Kuglin, K. F. Cuff, and R. L. Kortum, *Phys. Rev. Letters* **11**, 541 (1963).